A PARALLEL PARTICLE METHOD FOR SOLVING THE EEG SOURCE LOCALIZATION FORWARD PROBLEM

Ömer Demirel, Birte Schrader, and Ivo F. Sbalzarini

Institute of Theoretical Computer Science and Swiss Institute of Bioinformatics,
ETH Zurich, Universitätstr. 6, CH-8092 Zurich, Switzerland
phone: +(41) 44 632 63 44, fax: +(41) 44 632 15 62, email: ivos@ethz.ch
web: http://www.mosaic.ethz.ch

ABSTRACT

We present a parallel mesh-free particle method to solve the EEG forward problem in brain source localization. The method is based on discretization-corrected PSE operators and is entirely mesh-free. This allows the flexible representation of complex geometries and accurate solution of the forward problem inside and around them. We present the method and its parallel implementation, and we validate and benchmark it on a test problem for which the exact solution is known.

1. INTRODUCTION

Live visualization of electric brain activity is important in a diverse range of medical and biological applications, ranging from neurobiology to behavioral biology and psychology to personalized surgical planning, e.g., in epilepsy. Non-invasive methods include electroencephalography (EEG) and magnetoencephalography (MEG). These methods measure the distribution of the electric potential (in the case of EEG) or the magnetic field (in MEG) on the scalp surface or in the immediate vicinity of the head. Reconstructing from these measurements the internal brain activity that is most likely to have caused the observed surface distribution is an inverse problem. Accurate solutions depend on good regularization schemes. The problem is further complicated by the complex and patient-specific geometric shape of the brain, and by anatomical differences or lesions in the skull bone.

A first important step toward solving the source-localization problem is the development of a robust and accurate simulation of the forward problem. There, one is interested in predicting the expected potential or magnetic field distribution on the scalp from a known intracranial activity. This activity is hereby frequently modeled as an electric dipole [7, 12, 11, 20]. Knowing the position and orientation of the dipole, a numerical simulation is used to compute the potential on the scalp. Results from such simulations can then be used to regularize the inverse problem of localizing an unknown source from EEG or MEG measurements [4].

Previous works simulated the forward problem using Finite Element methods [21, 23, 20], Boundary Element Methods [8, 6], or Finite Difference methods [9]. Particular attention is usually given to the effects of anisotropic and inhomogeneous tissue conductivities and to the dipole-based modeling of the electric source currents in various head models [7, 12, 11]. Mesh-based simulation methods such as finite elements, however, may encounter stability problems or may become computationally inefficient in complex geometries, such as the human head and brain. The former is particularly pronounced for spectral elements, the latter stems from the fact that the system matrix can lose its band-diagonal structure in complex geometries, hence increasing the computational complexity of the solver. Moreover, generating a computational mesh in such geometries can be a daunting task in itself. Mesh-free simulations of the EEG forward problem have hence attracted growing interest [19].

Here, we present a novel mesh-free particle method for simulating the EEG forward problem. The method is based on discretization-corrected PSE operators [17]. PSE is a mesh-free discretization scheme for differential operators, first developed for diffusion operators [2] and later generalized to arbitrary differential operators [3]. It has previously been used for simulations in complex geometries [15] and on complex-shaped surfaces [14]. Recently, we have proposed a general discretization-correction (DC) framework for PSE operators [17], which allows using arbitrary particle distributions and remains consistent near boundaries. This allows more flexibility to place particles of various resolution in and around a geometric model of a brain or head as, e.g., segmented from 3D MRI or CT scan images. An example of a resulting particle distribution is shown in Fig. 1. In real simulations, however, a much larger number of particles is typically used, such that the simulation should efficiently parallelize over a multi-processor computer.

We use the Parallel Particle Mesh (PPM) Library [16,

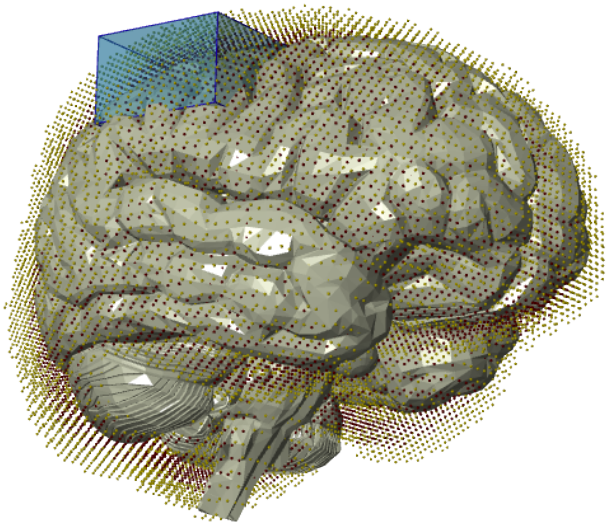

Figure 1: Illustration of a particle distribution around a geometric model of a human brain. Different colors indicate particles of different electrical conductivity. Here, red particles indicate skull bone, yellow ones scalp tissue and hair. For better visualization, only the geometric model of the brain is shown. The blue box indicates a region of interest for the measurements.

1] to implement a scalable and efficient parallel simulation. The PPM Library is a parallelization middleware for hybrid particle-mesh methods that provides automatic domain decomposition, load balancing, and communication scheduling. It has previously enabled simulations meeting or exceeding the performance of state-of-the-art hand-parallelized simulations [16, 13]. The PPM Library is based on a set of abstract parallel data structures and abstract operators for particle methods [13].

This paper is organized as follows: In Section 2, we briefly state the EEG forward problem and propose a novel particle method for its solution. In Section 3, we show validation results of the method on a simple test case where an analytical solution exists. Section 4 concludes the paper and outlines future work.

2. METHOD

In the EEG forward problem, we are given the locations and moments of a set of dipole current sources, an electrical conductivity field, and the head/brain geometry. We want to compute the electrical potential distribution on the scalp. This can be done by solving the quasi-static Maxwell equations of electromagnetism in the given geometry and conductivity field, using the dipoles as input current source. In EEG source analysis, quasi-static conditions hold [10, 5]. This is because the wavelength of the fastest electrical signals in the brain is much larger than the diameter of the head; we do not need to resolve transient electromagnetic waves. The non-magnetic part of the quasi-static Maxwell equations for volume conduction is:

$$\nabla \times \boldsymbol{E} = \boldsymbol{0}\,, \tag{1}$$

$$\nabla \cdot (\boldsymbol{\sigma} \boldsymbol{E}) = -\nabla \cdot \boldsymbol{J}_i\,, \tag{2}$$

where ∇ denotes the Nabla operator, $\boldsymbol{E}$ is the electric field, $\boldsymbol{J}_i$ is the source current density from the active dipoles, and $\boldsymbol{\sigma}(\boldsymbol{x})$ is the spatially varying electric conductivity tensor; $\boldsymbol{E}, \boldsymbol{J}_i \in \mathbb{R}^n, \sigma \in \mathbb{R}^{n\times n}$. Given the impressed current density $\boldsymbol{J}_i$, we solve for the electric potential Φ:

$$\boldsymbol{E} = -\nabla\Phi. \tag{3}$$

From Eq. 2, the electric potential $\Phi(\boldsymbol{x})$ at every location $\boldsymbol{x}$ in the head can be found by solving

$$\nabla \cdot (\boldsymbol{\sigma}\nabla\Phi) = \nabla \cdot \boldsymbol{J}_i\,. \tag{4}$$

The solution automatically also satisfies Eq. 1 because the curl of the gradient of any scalar field is always the zero vector. We find the solution to Eq. 4 by evolving an arbitrary initial field $\Phi_0(\boldsymbol{x})$ according to the partial differential equation

$$\frac{\partial\Phi}{\partial\tau} = \nabla \cdot (\boldsymbol{\sigma}\nabla\Phi) - \nabla \cdot \boldsymbol{J}_i \tag{5}$$

until steady state is reached. Here, τ can be understood as a pseudo-time; this evolution of Φ is not a physical process. Thus, instead of solving the general Poisson Eq. 4 by inverting the linear system of equations emerging from its spatial discretization, the anisotropic diffusion Eq. 5 is solved until steady state with an explicit time stepping scheme. This has the advantage that no global matrix needs to be inverted. The method is thus well suited to a parallel implementation. For isotropic conductivity, the conductivity tensor simplifies to a position-dependent scalar field.

Since no current can spontaneously exit the scalp and enter air, homogeneous Neumann boundary conditions are applied at the scalp:

$$\nabla\Phi \cdot \hat{\mathbf{n}} = 0\,, \tag{6}$$

where $\hat{\mathbf{n}}$ is the outward unit normal vector. The source current density $\boldsymbol{J}_i$ is usually modeled as a current dipole.

The evolution of Φ is performed on particles. The N particles, located at positions $\{\boldsymbol{x}_p\}_{p=1}^N$, carry the values $\Phi_p^0 = \Phi_0(\boldsymbol{x}_p)$, $\sigma_p = \sigma(\boldsymbol{x}_p)$, and $D_p = \nabla \cdot \boldsymbol{J}_i|_{\boldsymbol{x}_p}$. The values Φ_p^n are updated according to an explicit Euler time stepping scheme as:

$$\Phi_p^{n+1} = \Phi_p^n + \Delta t_p \left\{ [\nabla \cdot (\sigma\nabla\Phi)]_{p,h}^n - D_p \right\}, \tag{7}$$

where

$$[\nabla \cdot (\sigma \nabla \Phi)]^n_{p,h} = \frac{1}{2\varepsilon_p^2} \sum_q [\Phi^n_q - \Phi^n_p][\sigma_q + \sigma_q] K_p(\boldsymbol{x}_p - \boldsymbol{x}_q) \phi_{\varepsilon_p}(\boldsymbol{x}_p - \boldsymbol{x}_q) \tag{8}$$

is the DC PSE approximation of $\nabla \cdot (\sigma \nabla \Phi)$ at time step n and position $\boldsymbol{x}_p$. Here, ε_p is the particle-specific kernel width, K_p the particle-specific correction function, and ϕ the kernel window function (see Ref. [17] for details about the DC PSE method). The error of the approximation in Eq. 8 is of order $O(\varepsilon_p^2)$.

In order to avoid numerical difficulties caused by the infinite gradients at the dipole, we regularize the singularity using ideas presented by other authors [18, 19]. Moreover, at the borders between different tissues or materials, and on the surface of the scalp, the electrical conductivity jumps. These discontinuities are also regularized in order to achieve better numerical accuracy. Here, we directly use the DC PSE operators to regularize the conductivity field, leading to a consistent method.

In our simulations, we consider as the computational domain a box completely containing a head model. We apply DC PSE diffusion operators to smooth the initial σ-field to the resolution of the method. The resolution is defined by the DC PSE kernel width ε_p [17] and is set by the user. We choose kernel widths that are equal to the inter-particle spacing. Once the smoothed conductivity values are computed on each particle, we use DC PSE operators to compute the gradient of the smoothed conductivity and store it on the particles as well. After this initialization, the following algorithm is iterated at each time step:

1. Loop over all particles and apply the DC PSE operator for anisotropic diffusion (Eq. 8) to solve Eq. 5 to steady state.
2. Update Φ using an Euler time stepping scheme according to Eq. 7.
3. Compute the residual $R_e = \|\nabla \cdot (\sigma \nabla \Phi) - \nabla \cdot \boldsymbol{J}_i\|$.
4. If $R_e < R_{\max}$, the final solution Φ is found, else loop back to Step 1.

3. BENCHMARKS

We verify the consistency and accuracy of the present method in a simple test case where an analytical solution exists, the homogeneous spherical head model [22]. Historically, spherical head models have been widely used in solving the EEG forward problem. Even though these models fail to capture the geometry of a head or brain, they allow validation of newly developed simulation algorithms since analytical solutions for the EEG forward problem exist in this case [22].

We consider a sphere of radius R, centered at the origin and filled with a homogeneously conducting material with constant and scalar σ. Inside the sphere is a dipole, located at $\boldsymbol{r}_0 = (0.1, 0.1, 0.1)$ with dipole moment $\boldsymbol{m} = (1.0, 1.0, 1.0)$. The analytical solution for the electric potential Φ is known at every $\boldsymbol{r}$ for $r > r_0$:

$$\Phi = \frac{\boldsymbol{m}}{4\pi\sigma} \cdot \left\{ \frac{\boldsymbol{r} - \boldsymbol{r}_0}{r_p^3} + \frac{\left(\boldsymbol{r} - \frac{r^2}{R^2}\boldsymbol{r}_0\right)}{R^3 r_{pi}^3} + \frac{1}{R^3 r_{pi}} \left[\boldsymbol{r} + \frac{\boldsymbol{r}\frac{r_0 r}{R^2}\cos\varphi - \frac{r^2}{R^2}\boldsymbol{r}_0}{r_{pi} + 1 + \frac{r_0 r}{R^2}\cos\varphi} \right] \right\}, \tag{9}$$

where φ is the angle between $\boldsymbol{r}_0$ and $\boldsymbol{r}$, the displacement vector is $\boldsymbol{r}_p = \boldsymbol{r} - \boldsymbol{r}_0$ with length $r_p = \sqrt{(r^2 + r_0^2 - 2 r r_0 \cos\varphi)}$, and $r_{pi} = \sqrt{(1 + (\frac{r_0 r}{R^2})^2 - 2\frac{r_0 r}{R^2}\cos\varphi)}$. For a schematic illustration of $\boldsymbol{r}_{pi}$ please see Ref. [22].

The present method does not rely on regular particle distributions. In this benchmark, however, we place the particles at the nodes of a Cartesian lattice with resolution h, spanning the entire computational domain. This renders the convergence analysis simpler and more easily reproducible.

In order to minimize the deteriorating effect of the dipole and the smoothed conductivity region on the sphere surface, we define a control shell with inner radius $r_1 = \frac{9}{26}R$ and outer radius $r_2 = \frac{12}{26}R$. We use the above algorithm to simulate the electric potential everywhere in the sphere and on its surface. We then compare the so-obtained numerical solution with the exact analytical solution from Eq. 9. Figure 2 shows the L_2 and L_∞ norms of the relative errors of the numerical solution inside the control shell. The dotted line indicates second-order convergence. As expected from the second-order DC PSE kernels used, the simulation errors decrease quadratically with the inter-particle spacing h.

Figure 3 shows the resulting electric potential on the surface of the sphere as computed by the present method.

All simulations are run in parallel on a cluster of quad-core AMD Opteron 8380 CPUs where each node has four CPUs and 32 GB of RAM. The simulation is implemented as a client to the parallelization middleware PPM [16, 1] and has been tested on up to 64 distributed-memory processor cores. Figure 4 shows the parallel efficiency achieved by the present implementation of the method for weak scaling. The parallel efficiency measures the fraction of the CPU time spent doing productive computations. It is less than 1 and monotonically decreasing with increasing processor numbers as the communication and synchronization overhead grows. We compute the parallel efficiency from its definition:

$$e = \frac{t(1) N(N_{\text{Proc}})}{t(N_{\text{Proc}}) N(1) N_{\text{Proc}}},$$

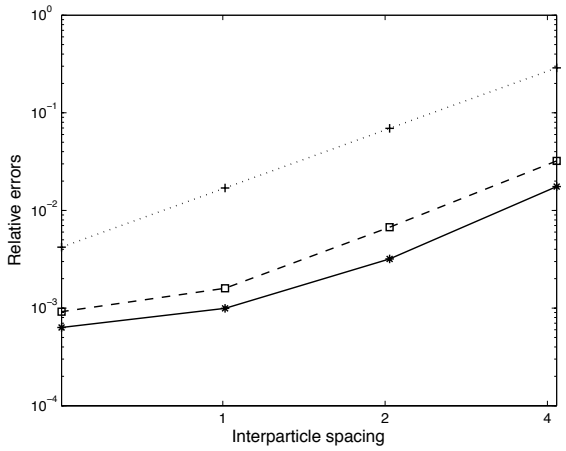

Figure 2: The convergence of the L_2 ($*$) and L_∞ ($\square$) norms of the relative errors of the numerical solution for the homogeneous spherical head test case with decreasing interparticle spacing h. The dotted line indicates second-order convergence.

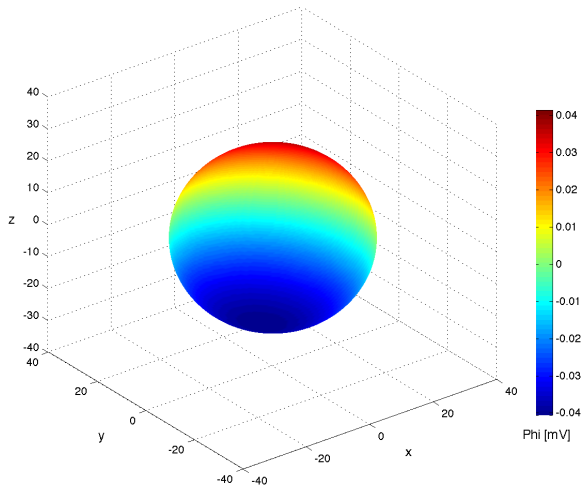

Figure 3: Visualization of the numerically computed electric potential, interpolated from the particles onto the surface of the sphere.

where $t(1)$ is the wall-clock time to solution on a single processor core, $t(N_{\text{Proc}})$ the time to solution when running in parallel on N_{Proc} processor cores, and $N(1)$ and $N(N_{\text{Proc}})$ are the problem sizes (numbers of particles) on 1 and N_{Proc} processor cores, respectively. The parallel efficiency on 64 processors was 0.88, indicating good scalability of the code to moderate numbers of processors as relevant to the present problem. All absolute wall-clock times were between 3 and 4 seconds per time step.

4. CONCLUSIONS

We have introduced a mesh-free particle method to solve the EEG forward problem. The presented method uses DC PSE operators in order to provide the maximum flexibility when placing the particles in and around complex head/brain geometries. We have presented the simulation algorithm and verified its consistency and convergence on a simple test problem for which an exact solution is available. The results show that the method converges with the proper order of accuracy. The simulation is implemented as a client to the PPM Library [16, 1], which allows it to run in parallel on multiple processors. We have benchmarked the implementation on up to 64 distributed-memory processor cores, showing parallel efficiencies better than 80%.

Ongoing and future work is concerned with testing the method on more realistic head models and head/brain geometries as segmented out of MRI or CT scans. This will also include validation of the method against experimentally measured EEG signals. The inherent adaptivity of the DC PSE particle method and the parallel software implementation using PPM are expected to be beneficial then. Future work will also extend the method to the MEG forward problem, for which the magnetic field needs to be simulated as well.

5. ACKNOWLEDGMENTS

We thank Dr. Sylvain Reboux, MOSAIC Group, ETH Zurich for many useful discussions and for his help with setting up the simulations. The present work is supported by two grants from the Swiss National Science Foundation (SNSF), grants #200021-132064 and #200021-115764, to I.F.S.

6. REFERENCES

[1] O. Awile, O. Demirel, and I. F. Sbalzarini. Toward an object-oriented core of the PPM library. In *Proc. ICNAAM, Numerical Analysis and Applied Mathematics, International Conference*, pages 1313–1316. AIP, 2010.

[2] P. Degond and S. Mas-Gallic. The weighted particle method for convection-diffusion equations. Part 2: The anisotropic case. *Math. Comput.*, 53(188):509–525, 1989.

[3] J. D. Eldredge, A. Leonard, and T. Colonius. A general deterministic treatment of derivatives in particle methods. *J. Comput. Phys.*, 180:686–709, 2002.

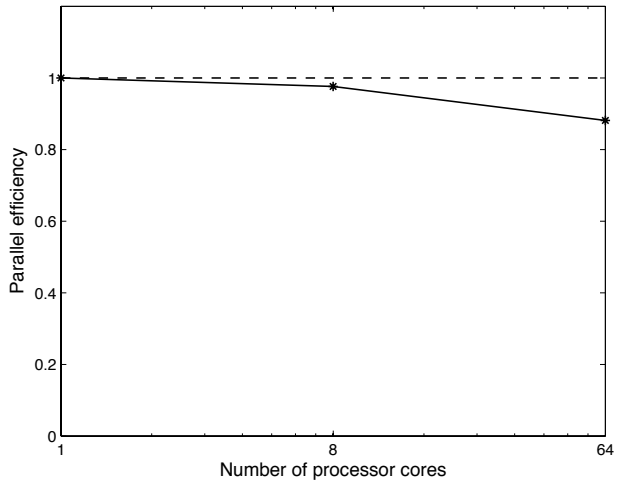

Figure 4: Parallel efficiency for a weak scaling starting from 32 000 particles on 1 processor and going up to 2.1 million particles on 64 processors.

[4] R. Grech, T. Cassar, J. Muscat, K. P. Camilleri, S. G. Fabri, M. Zervakis, P. Xanthopoulos, V. Sakkalis, and B. Vanrumste. Review on solving the inverse problem in EEG source analysis. *J. Neuroeng. Rehabil*, 5:25, 2008.

[5] H. Hallez, B. Vanrumste, R. Grech, J. Muscat, W. De Clercq, A. Vergult, Y. D'Asseler, K. P. Camilleri, S. G. Fabri, S. Van Huffel, and I. Lemahieu. Review on solving the forward problem in eeg source analysis. *Journal of NeuroEngineering and Rehabilitation*, 4:46–66, 2007.

[6] M. S. Hämäläinen and J. Sarvas. Realistic conductivity geometry model of the human head for interpretation of neuromagnetic data. *IEEE Trans. Biomed. Eng.*, 36(2):165–171, 1989.

[7] J. Haueisen, C. Ramon, M. Eiselt, H. Brauer, and H. Nowak. Influence of tissue resistivities on neuromagnetic fields and electric potentials studied with a finite element model of the head. *IEEE Trans. Biomed. Eng.*, 44(8):727, 1997.

[8] B. He, T. Musha, Y. Okamoto, S. Homma, Y. Nakajima, and T. Sato. Electric dipole tracing in the brain by means of the boundary element method and its solution accuracy. *IEEE Trans. Biomed. Eng.*, 34:406–414, 1987.

[9] L. Lemieux, A. McBride, and J. W. Hand. Calculation of electrical potentials on the surface of a realistic head model by finite differences. *Phys. Med. Biol.*, 41:1079–1091, 1996.

[10] R. Plonsey and D. B. Heppner. Considerations of quasi-stationarity in electrophysiological systems. *Bull. Math. Biophys.*, 29:657–664, 1967.

[11] C. Ramon, J. Haueisen, and P. H. Schimpf. Influence of head models on neuromagnetic fields and inverse source localizations. *Biomedical Engineering OnLine*, 5(55), 2006.

[12] C. Ramon, P. Schimpf, J. Haueisen, M. Holmes, and A. Ishimaru. Role of soft bone, CSF and gray matter in EEG simulations. *Brain Topogr.*, 16(4):245–248, 2004.

[13] I. F. Sbalzarini. Abstractions and middleware for petascale computing and beyond. *Intl. J. Distr. Systems & Technol.*, 1(2):40–56, 2010.

[14] I. F. Sbalzarini, A. Hayer, A. Helenius, and P. Koumoutsakos. Simulations of (an)isotropic diffusion on curved biological surfaces. *Biophys. J.*, 90(3):878–885, 2006.

[15] I. F. Sbalzarini, A. Mezzacasa, A. Helenius, and P. Koumoutsakos. Effects of organelle shape on fluorescence recovery after photobleaching. *Biophys. J.*, 89(3):1482–1492, 2005.

[16] I. F. Sbalzarini, J. H. Walther, M. Bergdorf, S. E. Hieber, E. M. Kotsalis, and P. Koumoutsakos. PPM – a highly efficient parallel particle-mesh library for the simulation of continuum systems. *J. Comput. Phys.*, 215(2):566–588, 2006.

[17] B. Schrader, S. Reboux, and I. F. Sbalzarini. Discretization correction of general integral PSE operators in particle methods. *J. Comput. Phys.*, 229:4159–4182, 2010.

[18] S. P. van den Broek, H. Zhou, and M. J. Peters. Computation of neuromagnetic fields using finite-element method and biot-savart law. *Med. Biol. Eng. Comput.*, 34:21–26, 1996.

[19] N. von Ellenrieder, C. H. Muravchik, and A. Nehorai. A meshless method for solving the EEG forward problem. *IEEE Trans. Biomed. Eng.*, 52(2):249–257, February 2005.

[20] C. H. Wolters, H. Köstler, C. Möller, J. Härdtlein, and A. Anwander. Numerical approaches for dipole modeling in finite element method based source analysis. *Internat. Congress Series*, 1300:189–192, 2007.

[21] Y. Yan, P. L. Nunez, and R. T. Hart. Finite-element model of the human head: scalp potentials due to dipole sources. *Med. Biol. Eng. Comput.*, 29(5):475–481, 1991.

[22] D. Yao. Electric potential produced by a dipole in a homogeneous conducting sphere. *IEEE Trans. Biomed. Eng.*, 47(7):964–966, 2000.

[23] Y. C. Zhang, S. A. Zhu, and B. He. A second-order finite element algorithm for solving the three-dimensional EEG forward problem. *Phys. Med. Biol.*, 49:2975–2987, 2004.